

Cite this article as: Li Yan, Chen Wenshuai, Zhou Zenglin, et al. Effect of Annealing Treatment on σ -Phase Characteristics of Mo-47.5Re Alloy Foil[J]. Rare Metal Materials and Engineering, 2023, 52(02): 433-440.

ARTICLE

Effect of Annealing Treatment on σ -Phase Characteristics of Mo-47.5Re Alloy Foil

Li Yan¹, Chen Wenshuai^{1,2,3}, Zhou Zenglin^{1,2,3}, He Xueliang¹, Hui Zhilin¹

¹ GRIMAT Engineering Institute Co., Ltd, Beijing 101407, China; ² State Key Laboratory of Advanced Materials for Smart Sensing, GRINM Group Co., Ltd, Beijing 100088, China; ³ General Research Institute for Nonferrous Metals, Beijing 100088, China

Abstract: Using powder metallurgy sintered billet as raw material, Mo-47.5Re (wt%) foils with the thicknesses of 0.035 and 0.030 mm were obtained by multi-pass rolling and intermediate annealing. After hydrogen annealing at 1300–1900 °C, metallurgical microscopy, SEM and EDS were used to analyze the effect of annealing temperature on characteristics of σ -phase. EDS analysis indicates that Mo:Re atomic ratio of second phase in the ND direction approaches to 1:1, and that in the RD direction is close to or lower than 1:2, so the majority of second phase in Mo-47.5Re foils is σ -phase; but Mo:Re atomic ratio of second phase in the RD direction is relatively low, even reaching 1:4. The micrograph characteristics of Mo-47.5Re foil includes large grains, few deformation twins, and larger and more σ -phase particles in grains than at the grain boundary. The number of σ -phase in 0.035 and 0.030 mm thick foils increases first and then decreases with raising annealing temperature. After annealing at 1300 °C, σ -phase number of 0.035-mm-sample reaches the maximum and the grain size is significantly reduced, while 0.030-mm-sample shows this phenomenon at 1500 °C. After annealing at 1900 °C, a few small-sized σ -phase particles remain in the RD direction of 0.030-mm-sample, and all σ -phase particles in the ND direction of 0.030-mm-sample and those in RD and ND directions of 0.035-mm-sample are totally redissolved and disappear. In as-rolled and relatively low-temperature annealed samples, such as 1300 °C, most σ -phase particles have irregular polygonal morphology, and a few of them are spherical. After annealing at 1500 °C and higher temperatures, σ -phase particles in some samples exhibit a cube shape.

Key words: Mo-47.5Re foil; rolling; σ -phase; annealing temperature; micromorphology

For the purpose of simultaneously obtaining high strength-plasticity^[1–7] and improving the processing and performance of molybdenum materials^[8–14], molybdenum-rhenium alloy was successfully developed and reported by Geach and Hughes in 1955^[15–16]. Molybdenum-rhenium foil is a kind of functional and structural material which has been widely used in radar, communication and other electronic fields. Functionally, the electrical properties and high temperature resistance of the material are mainly used. As a structural material, it is favored mainly because of high temperature strength and room temperature plasticity, especially after high temperature or even ultra-high temperature service and recrystallization, the material can still maintain good room temperature plasticity^[17–18].

It has been shown in Ref. [19] that with the increase in rhenium content, especially 40wt% and above, high-temperature strength, low-temperature plasticity and thermal

shock resistance of high-rhenium molybdenum alloys are significantly improved.

Combining molybdenum-rhenium alloy thermo-dynamic model established by first-principle calculations^[20] and microstructure observations, we found that molybdenum is solid-dissolved in rhenium and forms a hexagonal close-packed β -phase; when rhenium content exceeds 45wt%, the β -phase and the liquid undergo a peritectic reaction^[21], and the σ -phase with tetrahedral structure (MoRe₂, structure type D8₆, space group P4₂/mnm, lattice constant $a=0.9579$ nm, $c=0.4974$ nm) will be preferentially precipitated at the grain boundaries^[22–23]. σ -phase is an intermetallic compound with high strength and high hardness. In addition, although it is indicated that the presence of a small amount of σ -phases will not cause the consequence of precipitation hardening of molybdenum alloy containing 41wt% and 47.5wt% rhenium, an excessive content of σ -phase will adversely affect the

Received date: April 21, 2022

Foundation item: National Key R&D Program of China (2017YFB0306000)

Corresponding author: Zhou Zenglin, Ph. D., Professor, GRIMAT Engineering Institute Co., Ltd, Beijing 101407, P. R. China, Tel: 0086-10-60662616, E-mail: zhouzenglin@grimm.com

Copyright © 2023, Northwest Institute for Nonferrous Metal Research. Published by Science Press. All rights reserved.

plasticity of the alloy^[24]. σ -phase has a complex tetragonal lattice. The specific volume of each crystal structure is almost half that of the matrix, and the lattice parameter ($a=0.9579$ nm) in tetragonal direction is more than three times larger than that of the matrix ($a=0.3141$ nm). These characteristics of σ -phase make it impossible to nucleate uniformly. Therefore, new crystals must be formed preferentially at the defect. The habit plane of the precipitate is $\{110\}$ of the matrix, and the orientation relationship between the precipitate and the substrate is that the precipitate (100) is parallel to the substrate (100)^[25].

Therefore, σ -phase is a decisive factor for the excellent properties of high rhenium molybdenum-rhenium alloys, and its influence on the alloy properties depends largely on the morphology and distribution of its nucleation and precipitation during plastic working and heat treatment. However, due to high cost of metal rhenium, the application of molybdenum rhenium alloys is concentrated in specific fields such as aerospace and nuclear industry. At present, there are relatively few studies on molybdenum-rhenium alloys with high rhenium content, and most of them focus on the specific properties of the alloy. The research on microstructure, especially the characteristics include content, size, morphology and distribution of σ -phase inside the alloy is relatively lacking. In this study, Mo-47.5Re (wt%) foils with thicknesses of 0.035 and 0.030 mm obtained by powder metallurgy pressing, sintering and rolling deformation were annealed at different temperatures, and the influence of annealing temperature on the content, size, morphology and distribution of σ -phase in the alloy and its mechanism were studied.

1 Experiment

1.1 Experimental materials

Mo-47.5Re (wt%) slabs with a thickness of 10 mm prepared by powder metallurgy technology was processed by multiple passes of hot rolling, warm rolling, cold rolling and intermediate annealing to obtain 0.035 mm \times 60 mm \times 300 mm (referred to as 0.035-mm-sample) and 0.030 mm \times 60 mm \times 300 mm (referred to as 0.030-mm-sample) two rolled molybdenum-rhenium foils.

1.2 Annealing treatment

Molybdenum-rhenium foils with different thicknesses were annealed in a vacuum-hydrogen high temperature furnace. The temperature parameters were set as 1300, 1500, 1700 and 1900 °C. The heating rate was 10 °C/min, and holding time was 60 min. Subsequently the temperature was reduced to 1200 °C at 25 °C/min, and then the samples were cooled with the furnace.

1.3 Metallographic and SEM analysis

The metallographic and SEM samples of 8 mm \times 10 mm (length \times width) were cut along the rolling direction (RD) and the normal direction (ND) using a CNC wire-cutting machine. Because the sample B is thin, a copper sheet must be attached to the back of the sample in order to ensure the flatness, then

ground and polished. And then the sample was corroded with an aqueous solution of 10wt% NaOH+10wt% Fe (KCN)₃ for 2 min. A metallographic microscope (Zeiss Axiovision 200 MAT) was used to observe the microstructure of the sample, and the composition and element distribution of σ -phase were analyzed by EDS. Characterization of size distribution of σ particle was conducted by Nano Measurer analysis software. The crystal structure model of σ -phase was constructed by Crystalmaker.

1.4 Microhardness test

The micro-Vickers hardness of molybdenum-rhenium foils before and after annealing was measured by digital micro-Vickers hardness tester (VTD405, Beijing Woweii). After the sample was inlaid, the sandpaper was used for grinding and polishing to remove the oxide and oil pollution on the surface, and then the hardness value was measured. The selected test load was 25 g and the loading time was 10 s.

2 Results and Discussion

2.1 Composition analysis of second phase in different directions

Through the Mo-Re phase diagram, it can be found that although the theoretical chemical formula of σ -phase is generally marked as MoRe₂, in fact, Mo:Re can be ranged from 1:1 to 2:5. As shown in Fig. 1c and 1d, we performed EDS spot scan analysis on the σ -phase in the ND and RD of Mo-47.5Re alloy which is as rolled and annealed at different temperatures. The composition analysis results of the second phase in RD and ND of samples with two thicknesses and different processing conditions by EDS are shown in Fig. 1a.

According to the data comparison, the Mo:Re atomic ratio of second phase in ND of most samples is close to or slightly higher than 1:1, while that in RD is close to or lower than 1:2, so most of the second phase particles in molybdenum-rhenium foil are σ -phases. But obviously, the Mo:Re atomic ratio of second phase in the RD is relatively lower, even reaching 1:4.

As shown in Fig. 1b, the σ -phase in molybdenum-rhenium alloy is tetrahedral crystal structure. After rolling with large deformation, σ -phases in the ND and RD show different crystal orientations and compositional anisotropy is obtained^[26].

2.2 σ -phase characteristics of as-rolled materials

Fig. 2 shows the ND metallographic microstructure of two as-rolled molybdenum-rhenium foils with 0.035 and 0.030 mm in thicknesses. It can be seen that the grain size of two molybdenum-rhenium alloy foils is relatively large, and a large number of σ -phase particles are distributed in the grain and at the grain boundary. Compared with grain interior, grain boundary is the preferred location for the nucleation and precipitation of second phase. However, in this experiment, σ -particle number in the grain is far larger than that at the grain boundary. On the one hand, compared with that of fine grains, the grain boundary volume of coarse grains decreases, and thus it is difficult for the grain boundaries to provide more

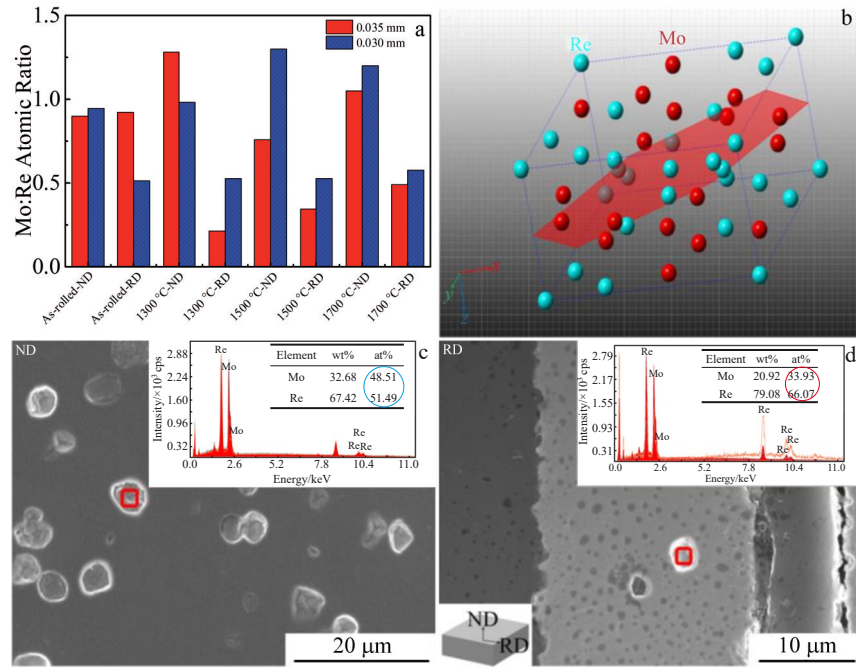


Fig.1 Atomic ratios of Mo:Re (a), crystal structure (b), and EDS analysis of σ -phase in ND (c) and RD (d) of molybdenum-rhenium foils

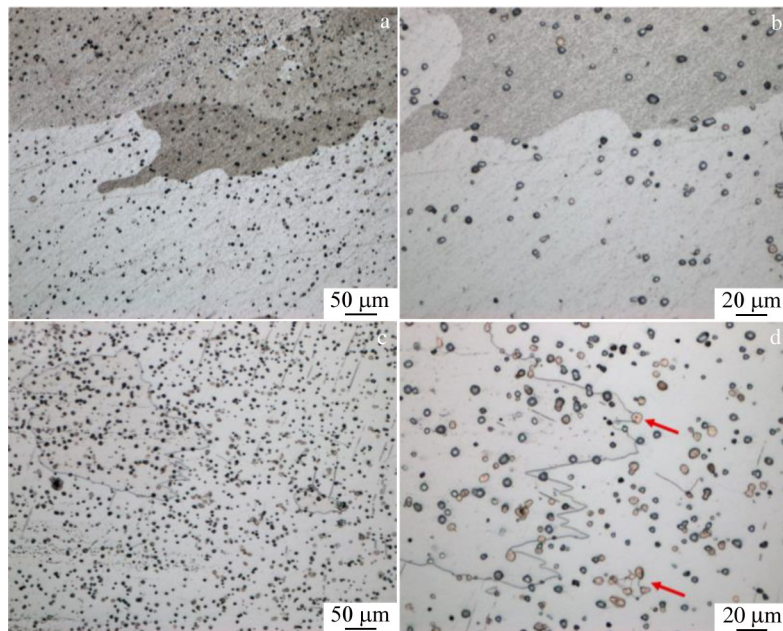


Fig.2 Metallographic microstructures of as-rolled samples with 0.035 mm (a, b) and 0.030 mm (c, d) in thickness in the ND

nucleation and growth space for σ -phase. On the other hand, a large number of structures with high defect concentration such as dislocations are generated inside the sample after rolling with large deformation. These structures provide a rapid diffusion channel to transport and to help the nucleation and growth of the second phase^[27]. In addition, the microstructure of the two samples does not show obvious fibrous shape, which is common after rolling deformation. The number of deformed twins is small, the grain size is large, and the grain boundaries are irregular. As shown by the red arrow in Fig.2d, the grain boundary presents a zigzag shape, and there are

scattered σ -phase particles at the grain boundary, indicating that the hard second phase generated acts as a pinning hindrance to grain boundary migration, thereby limiting grain growth to a certain extent and strengthening the macroscopic mechanical properties of the material^[28]. Moreover, σ particles in ND of 0.030-mm-sample are obviously more than that of 0.035-mm-sample, indicating that the increase in the deformation promotes the precipitation of σ -phase in the ND. So the stress and strain are also important driving forces for the precipitation of σ -phase.

The SEM morphologies of σ -phase of 0.035 and 0.030 mm

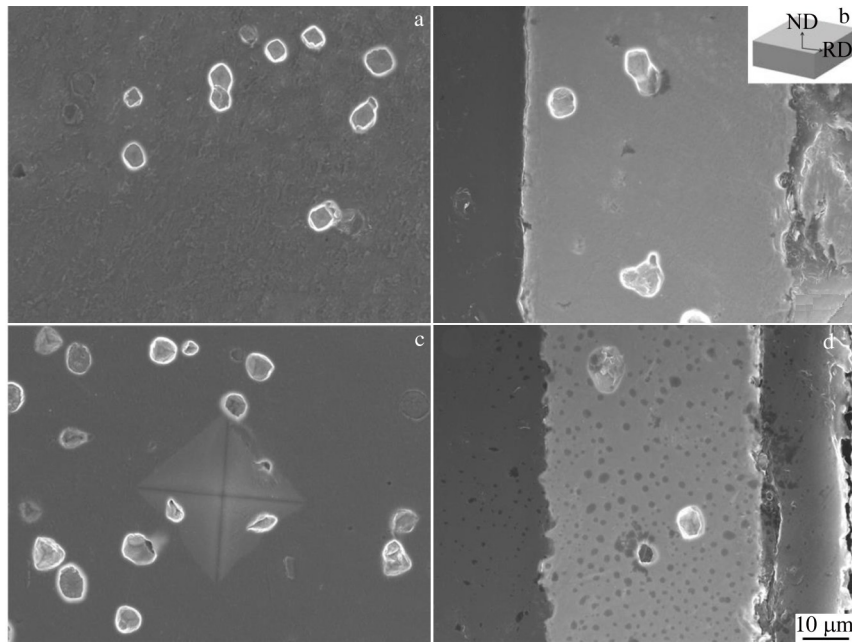


Fig.3 σ -phase morphologies of 0.035 mm (a, b) and 0.030 mm (c, d) as-rolled samples in ND (a, c) and RD (b, d)

as-rolled samples in the ND and RD are shown in Fig. 3. Similarly, the number of σ -phases in the ND of 0.030-mm-sample is significantly larger than that of 0.035-mm-sample, and most of the second phases are shaped like irregular polygons. Combined with the measurement results of Nano Measurer analysis software, the size of σ particle in 0.035-mm-samples is concentrated in 3.6–4.6 μm , and that in 0.030-mm-samples is concentrated in 3.8–5.5 μm , indicating that σ particles' size in the samples with two different deformation amounts is similar, but the size of σ particles in 0.035-mm-samples is relatively smaller.

2.3 Effect of annealing temperature on size, quantity and distribution of σ -phase

As shown in Fig.4, σ -phase varies in the ND of 0.035-mm-sample with the annealing temperature. After annealing at 1300 °C, a large number of small-sized σ particles are distributed inside the sample. Compared with the as-rolled samples, σ particle number is significantly increased and reaches the peak value, but the size is significantly decreased, concentrated in the range of 1.5–2.2 μm , reduced by about 55%, and there is also a small amount of larger-sized σ

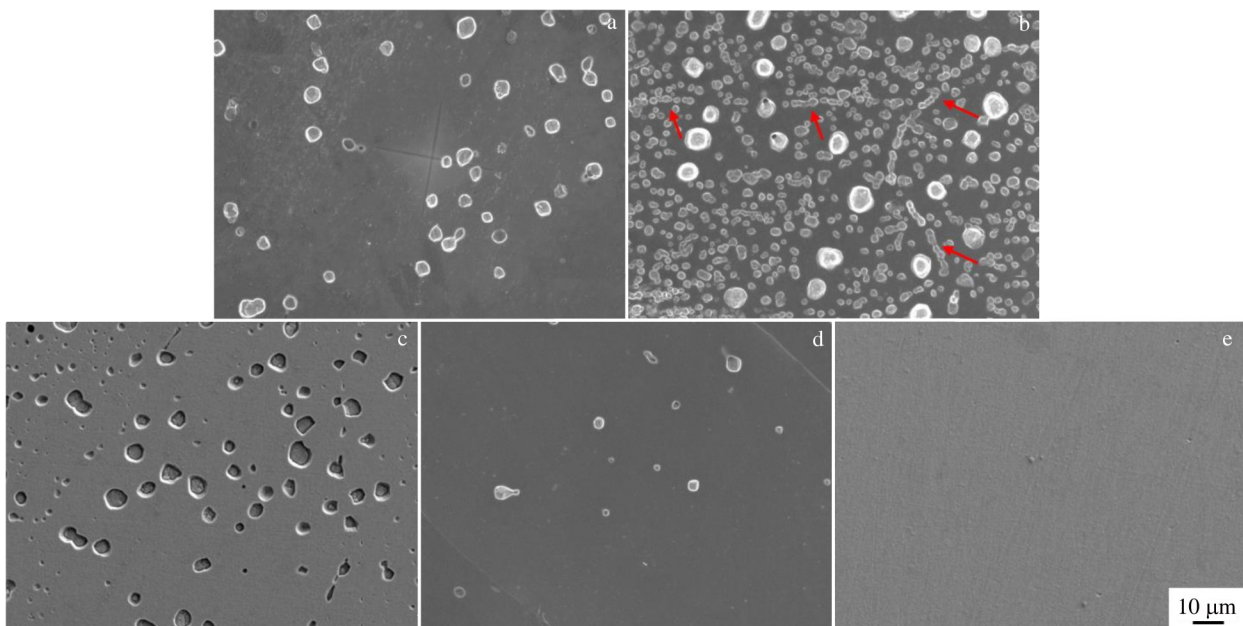


Fig.4 σ -phase in the ND of 0.035-mm-sample at different annealing temperatures: (a) as-rolled, (b) 1300 °C, (c) 1500 °C, (d) 1700 °C, and (e) 1900 °C

particles dispersed inside the sample. The grain boundaries are almost covered by a chain of small-sized σ particles, as shown by the red arrow in Fig.4b. It indicates that when the internal stress of the sample is high enough, the substructure that promotes pipeline diffusion inside, such as dislocation, is increased. The heterogeneous decomposition caused by temperature will lead to the nucleation and growth of secondary precipitates through diffusion, which is mainly along the wide dislocation channel pipeline, so the σ particle number increases significantly^[24]. Combined with Table 1, the micro-Vickers hardness of the material after annealing at 1300 °C is decreased by 10.9%, indicating that a more obvious recovery process occurs inside the sample, and σ -phase is also re-arranged. It can be seen from Table 2 that after annealing at 1500 °C, a large number of small-sized σ particles either gradually redissolve and disappear, or merge into larger-sized σ particles. Therefore, in this state, the interior of the sample is dominated by larger-sized σ particles whose size is concentrated in the range of 4.5–5.5 μm and much larger than 3.6–4.6 μm in rolled samples, and a small amount of the smaller σ particles remain around them. After annealing at 1700 °C, σ particles' size in the sample is concentrated in the range of 1.4–2.2 μm , and the number is

Table 1 Micro-Vickers hardness ($\times 9.8$ MPa) in ND and RD of as-rolled and 1300 °C-annealed samples

Direction	0.035-mm-sample		0.030-mm-sample	
	As-rolled	1300 °C-annealed	As-rolled	1300 °C-annealed
ND	440.5	392.6	461.5	448.9
RD	409.6	392.5	434.5	404.6

Table 2 Size distribution of σ -phase in ND of 0.035-mm-sample and 0.030-mm-sample at different annealing temperatures (μm)

Sample thickness/mm	As-rolled	1300 °C	1500 °C	1700 °C	1900 °C
0.035	3.6–4.6	1.5–2.2	4.5–5.5	1.4–2.2	-
0.030	3.8–5.5	3.8–6.0	2.2–3.1	2.2–3.4	-

significantly reduced. After annealing at 1900 °C, σ -phases in the ND direction in the sample are totally redissolved and disappear.

Compared with that of 0.035-mm-sample, σ -phase in the ND of 0.030-mm-sample has different variation characteristics with the annealing temperature, as shown in Fig. 5. The σ particles' number and size do not change significantly after annealing at 1300 °C, and the size distribution is still concentrated in 3.8–6.0 μm . The micro-Vickers hardness in the ND of 0.030-mm-sample is only reduced by 2.7% after annealing at 1300 °C, which is not significant compared with 10.9% of 0.035-mm-sample in Table 1. The results show that the internal microstructure of the sample does not change significantly after annealing at 1300 °C and the sample has high structural stability and strong annealing resistance. After annealing at 1500 °C, the micromorphology of σ particles changes obviously. The σ particle number increases distinctly and reaches a peak, but the size of most σ particles is obviously reduced, concentrated in 2.2–3.1 μm , and the size is decreased by about 42%. A small amount of large-sized σ particles is retained and dispersed in the grain. A chain of small-sized σ particles are also distributed at the grain boundaries, as shown by the red arrow in Fig. 5c. After

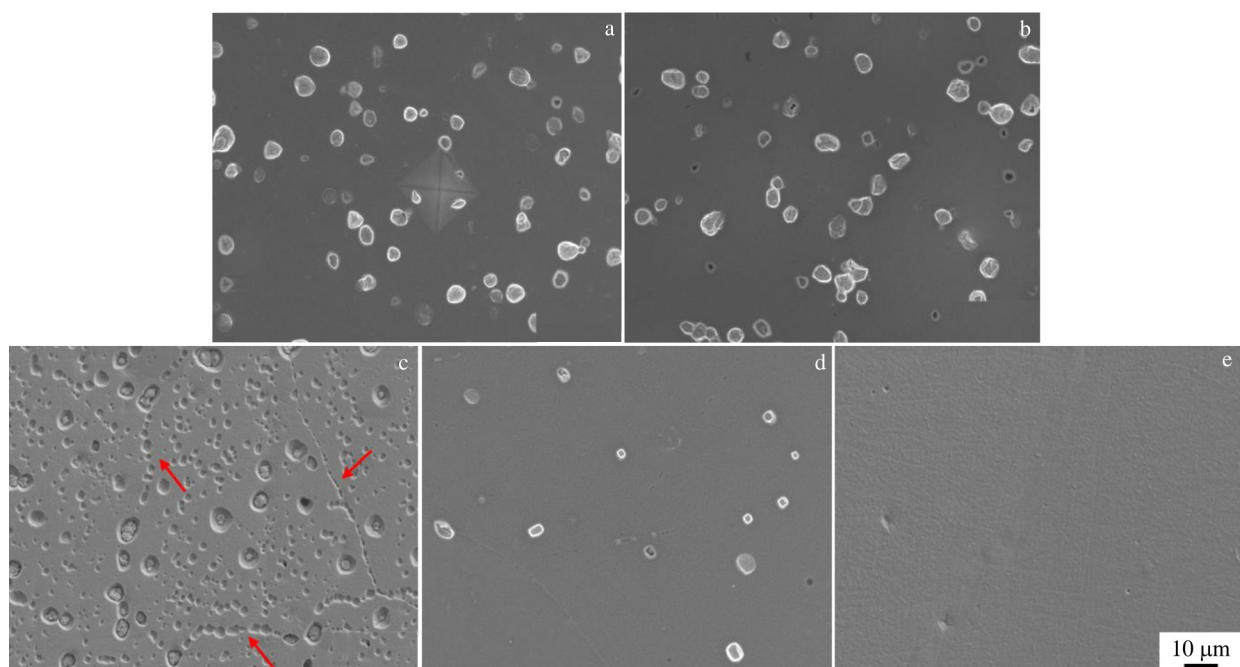


Fig. 5 σ -phase in the ND of 0.030-mm-sample at different annealing temperatures: (a) as-rolled, (b) 1300 °C, (c) 1500 °C, (d) 1700 °C, and (e) 1900 °C

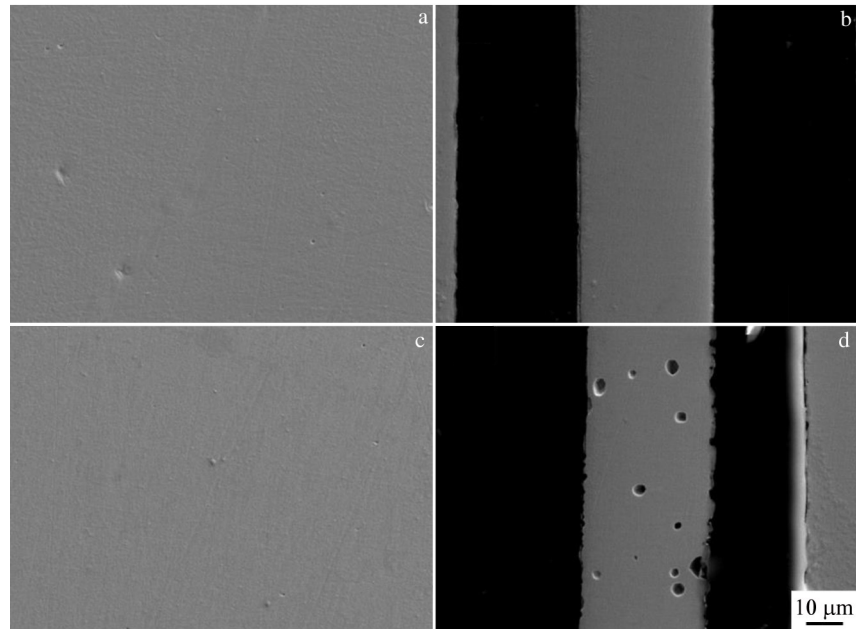


Fig.6 Morphologies in ND (a, c) and RD (b, d) of 0.035-mm-sample (a, b) and 0.030-mm-sample (c, d) annealed at 1900 °C

annealing at 1700 °C, the σ particle number in the foil is evidently reduced, but the size does not change significantly and is still concentrated in 2.2–3.4 μm . After annealing at 1900 °C, σ -phases in the ND are also redissolved and disappear completely.

The microstructures of the two samples in different directions after annealing at 1900 °C are shown in Fig.6. It can be seen that σ -phases in the ND and RD of 0.035-mm-sample and those in the ND of 0.030-mm-sample are all redissolved and disappear, while there are a small amount of small-sized σ particles left in the RD of 0.030-mm-sample. It is indicated that in the case of complete recrystallization with only a small number of defects and other substructures, the alloy needs to be slowly diffused for a long time to effectively homogenize the alloy composition^[24].

Fig.7 shows the position of σ -phase in the phase diagram of Mo-Re alloy after annealing at different temperatures, and compares it with the phase equilibrium of Mo-Re alloy obtained by first-principle and experimental research. On the one hand, it provides more sufficient and intuitive evidence for previous research work. On the other hand, in the bcc phase region of the phase diagram, we can still observe the existence of σ -phase, which also has a certain reference value for the improvement of the phase equilibrium of Mo-Re alloy.

2.4 Effect of annealing temperature on morphological characteristics of σ -phase

In this experiment, it is found that σ -phase exhibits different morphological characteristics after annealing at different temperatures. As shown in Fig. 8, most of σ -phase particles in the as-rolled and relatively low temperature annealed (1300 °C) samples show irregular polygonal morphology, and a small number of particles show spherical shape. After annealing at 1500 °C or above, nearly cubic σ -phase particles

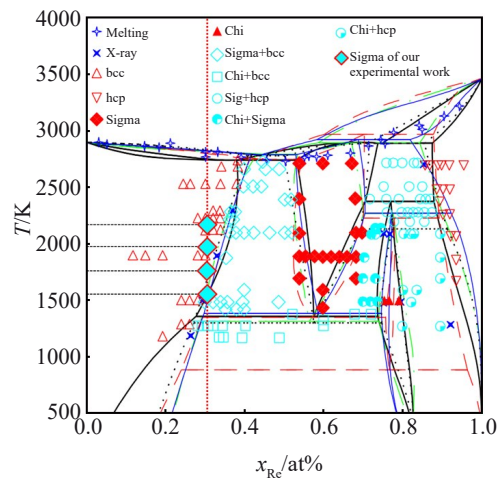


Fig.7 Comparison between the calculated Mo-Re phase diagram (in red edge blue bottom) with previous descriptions from Mathieu^[23]

appear in some samples, indicating that the increase in annealing temperature also affects the morphology of σ -phase.

2.5 Effect of annealing temperature on alloy properties

Through the room temperature tensile tests of alloy foils annealed at different temperatures, it is found that the change of σ -phase characteristics with annealing temperature is directly related to mechanical properties of Mo-47.5Re alloy. The tensile strength of the as-rolled 0.035-mm-samples and 0.030-mm-samples is higher than 840 MPa, and the fracture elongation is in the range of 2.5%–3.5%; after annealing at low temperatures of 1300–1500 °C, the tensile strength of the samples is still 750–800 MPa; but after annealing at higher temperatures of 1700–1900 °C, the tensile strength of the samples is significantly reduced to 610–640 MPa, but the

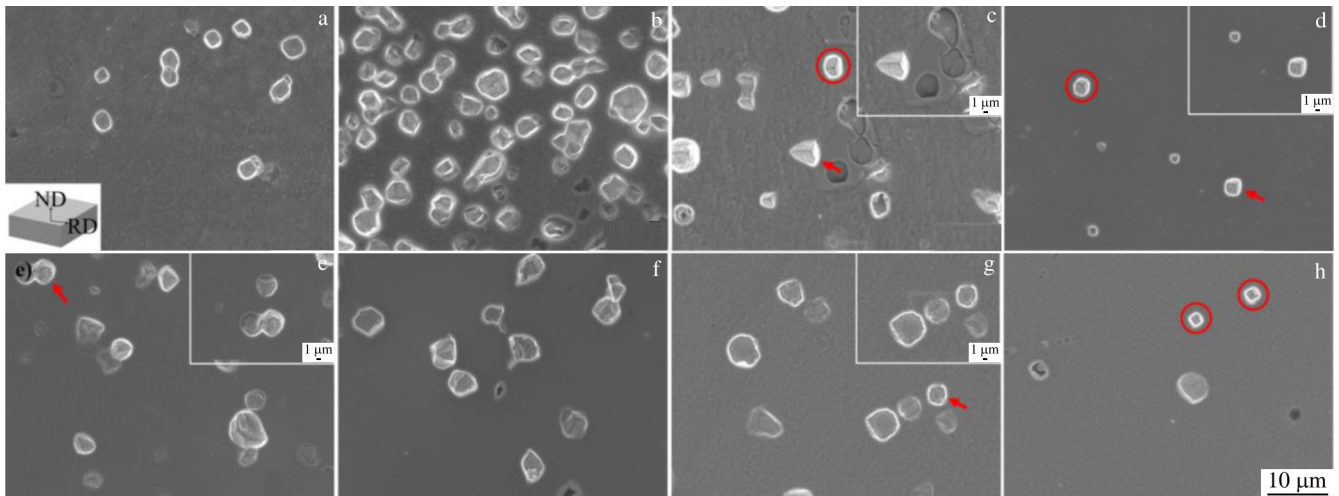


Fig.8 Micromorphologies of σ -phase in ND of 0.035-mm-samples (a–d) and 0.030-mm-samples (e–h) at different annealing temperatures: (a, e) as-rolled, (b, f) 1300 °C, (c, g) 1500 °C, and (d, h) 1700 °C

fracture elongation increases to 5.0% – 6.5%. From the discussion in the previous section, it can be concluded that the σ -phase will redissolve when annealed at 1500 °C and above. Therefore, it can be preliminarily inferred that the redissolution of the σ -phase caused by the change of the annealing process has a significant effect on the tensile strength of the alloy foil, but elongation is not sensitive to this.

3 Conclusions

1) Under the experimental conditions, the Mo:Re atomic ratio of the second phase in the ND of most molybdenum-rhenium foil samples is close to or higher than 1:1, and that in the RD is close to or lower than 1:2. So most of the second phase particles are σ -phase. But the Mo:Re atomic ratio of the second phase in the RD is lower, even reaching 1:4 individually. This may be related to different crystal orientations in two directions of the foils after rolling with a large amount of deformation.

2) The microstructures of two rolled foil samples show the characteristics of large grain size, few deformation twins, and σ -phase with large number and size, and there are more σ -phase particles inside the grain than at the grain boundary. σ -phase in the ND of 0.030-mm-sample is obviously more than that of 0.035-mm-sample, indicating that stress and strain are important driving forces for the precipitation of σ -phase.

3) The σ -phase number in 0.035-mm-samples and 0.030-mm-samples increases first and then decreases with raising the annealing temperature. After 0.035-mm-sample is annealed at 1300 °C, σ -phase number reaches the maximum, but the size is significantly decreased, and the similar phenomenon of 0.030-mm-sample appears after annealing at 1500 °C. After annealing at 1900 °C, a few small-sized σ particles remain in the RD of 0.030-mm-sample, and all σ -phases in the ND of 0.030-mm-sample and in the RD and ND directions of 0.035-mm-sample are completely redissolved and disappear. The analysis shows that besides stress and

strain, the temperature is another important driving force for the precipitation of σ -phase. And it is also proved that the slow dissolution and diffusion process of σ -phase can be effectively controlled by high temperature annealing when the molybdenum-rhenium foil is processed to a thinner size, that is, the internal energy storage is high enough.

4) Most of σ -phase particles in the molybdenum-rhenium foil presents an irregular polygonal morphology, and small part of them is spherical. After annealing at a higher temperature of 1500 °C and above, some σ particles exhibit a cube shape.

References

- 1 Gapontseva T M, Degtyarev M V, Voronova L M et al. *International Journal of Refractory Metals and Hard Materials*[J], 2021, 94: 105 389
- 2 Xing H R, Hu P, Zhou Y H et al. *Materials Characterization*[J], 2020, 165: 110 357
- 3 Li X, Zhang L, Wang G et al. *International Journal of Refractory Metals and Hard Materials*[J], 2020, 92: 105 294
- 4 Zhou Zenglin, Li Yan, Xie Yuanfeng et al. *Rare Metal Materials and Engineering*[J], 2019, 48(8): 2502 (in Chinese)
- 5 Braun J, Kaserer L, Stajkovic J et al. *International Journal of Refractory Metals and Hard Materials*[J], 2019, 84: 104 999
- 6 Leitner K, Lutz D, Knabl W et al. *Scripta Materialia*[J], 2018, 156: 60
- 7 Trinkle D R, Woodward C. *Science*[J], 2005, 310(5754): 1665
- 8 Caillard D. *Acta Materialia*[J], 2020, 194: 249
- 9 Harimon M A, Hidayati N A, Miyashita Y et al. *International Journal of Refractory Metals and Hard Materials*[J], 2017, 66: 52
- 10 Huang Hongtao, Wang Weijun, Zhong Wuye et al. *Atomic Energy Science and Technology*[J], 2020, 54: 505 (in Chinese)
- 11 Davidson D L. *Materials Science and Engineering A*[J], 2000,

- 293(1-2): 281
- 12 Medvedeva N I, Gornostyrev Y N, Freeman A J. *Physical Review B*[J], 2005, 72(13): 134 107
- 13 Xu Kedian. *Material Science and Engineering of Molybdenum*[M]. Beijing: Metallurgical Industry Press, 2014: 411 (in Chinese)
- 14 Wang Miao, Yang Shuangping, Liu Haijin et al. *Rare Metal Materials and Engineering*[J], 2021, 50(9): 3158
- 15 Geach G A, Hughes J E. *Plansee Proceedings*[C]. London: Pergamon Press, 1955: 245
- 16 Morito F. *JOM*[J], 1993, 45(6): 54
- 17 Leonhardt T, Carlén J C, Buck M et al. *AIP Conference Proceedings*[J], 1999, 458(1): 685
- 18 Fischer B, Freund D. *Metal Powder Report*[J], 2001, 56: 39
- 19 Yu X J, Kumar K S. *Materials Science and Engineering A*[J], 2016, 676: 312
- 20 Mao P, Han K, Xin Y. *Journal of Alloys and Compounds*[J], 2008, 464(1-2): 190
- 21 Yang Y, Zhang C, Chen S et al. *Intermetallics*[J], 2010, 18(4): 574
- 22 Garin J L, Mannheim R L. *Key Engineering Materials*[J], 2001, 189-191: 394
- 23 Mathieu R, Dupin N, Crivello J C et al. *Calphad*[J], 2013, 43: 18
- 24 Ogawa K, Maddin R. *Acta Metallurgica*[J], 1964, 12(10): 1161
- 25 Carlen J C, Bryskin B D. *Journal of Materials Engineering and Performance*[J], 1994, 3(2): 282
- 26 Shields Jr J A. *AIP Conference Proceedings*[J], 2005, 746(1): 835
- 27 Li Z, Wang J, Huang H. *Journal of Alloys and Compounds*[J], 2020, 818: 152 848
- 28 Kocks U F, Tome C N, Wenk H R. *Texture and Anisotropy*[M]. London: Cambridge University Press, 2000: 19

退火处理对Mo-47.5Re合金箔材 σ 相显微形貌的影响

李 艳¹, 陈文帅^{1,2,3}, 周增林^{1,2,3}, 何学良¹, 惠志林¹

(1. 有研工程技术研究院有限公司, 北京 101407)

(2. 有研科技集团有限公司 智能传感功能材料国家重点实验室, 北京 100088)

(3. 北京有色金属研究总院, 北京 100088)

摘要: 以粉末冶金烧结坯为原料, 通过多道次轧制和中间退火得到厚度分别为0.035和0.030 mm的Mo-47.5Re箔材(质量分数, %)。在1300~1900 °C氢气退火后, 采用金相显微镜、扫描电镜和能谱分析仪分析了退火温度对 σ 相特性的影响。EDS分析表明: 第二相的Mo:Re原子比在ND方向接近1:1, 在RD方向接近或低于1:2, 因此Mo-47.5Re箔内绝大多数第二相是 σ 相; 但RD方向第二相的Mo:Re原子比相对较低, 甚至接近1:4。钼铼合金箔材的特点是晶粒大、变形孪晶少、晶粒中的 σ 相颗粒比晶界处尺寸大、数量多。随着退火温度的升高, 0.035和0.030 mm厚箔材中 σ 相的数量先增加后减少。1300 °C退火后, 0.035 mm箔材的 σ 相数量达到最大值, 尺寸显著减小, 而0.030 mm样品在1500 °C退火后出现这种现象。1900 °C退火后, 0.030 mm样品的RD方向残留少量小尺寸 σ 相颗粒, ND方向和0.035 mm样品的RD和ND方向的 σ 相颗粒全部重新回溶并消失。在轧制态和相对低温退火样品中, 如1300 °C, 大部分 σ 相颗粒为不规则的多边形形貌, 少数为球形。在1500 °C及更高温度下退火后, 一些样品中的 σ 相颗粒呈立方体形貌。

关键词: Mo-47.5Re合金; 轧制变形; σ 相; 退火温度; 显微形貌

作者简介: 李 艳, 女, 1979年生, 博士, 正高级工程师, 有研工程技术研究院有限公司, 北京 101407, E-mail: liy@grinm.com